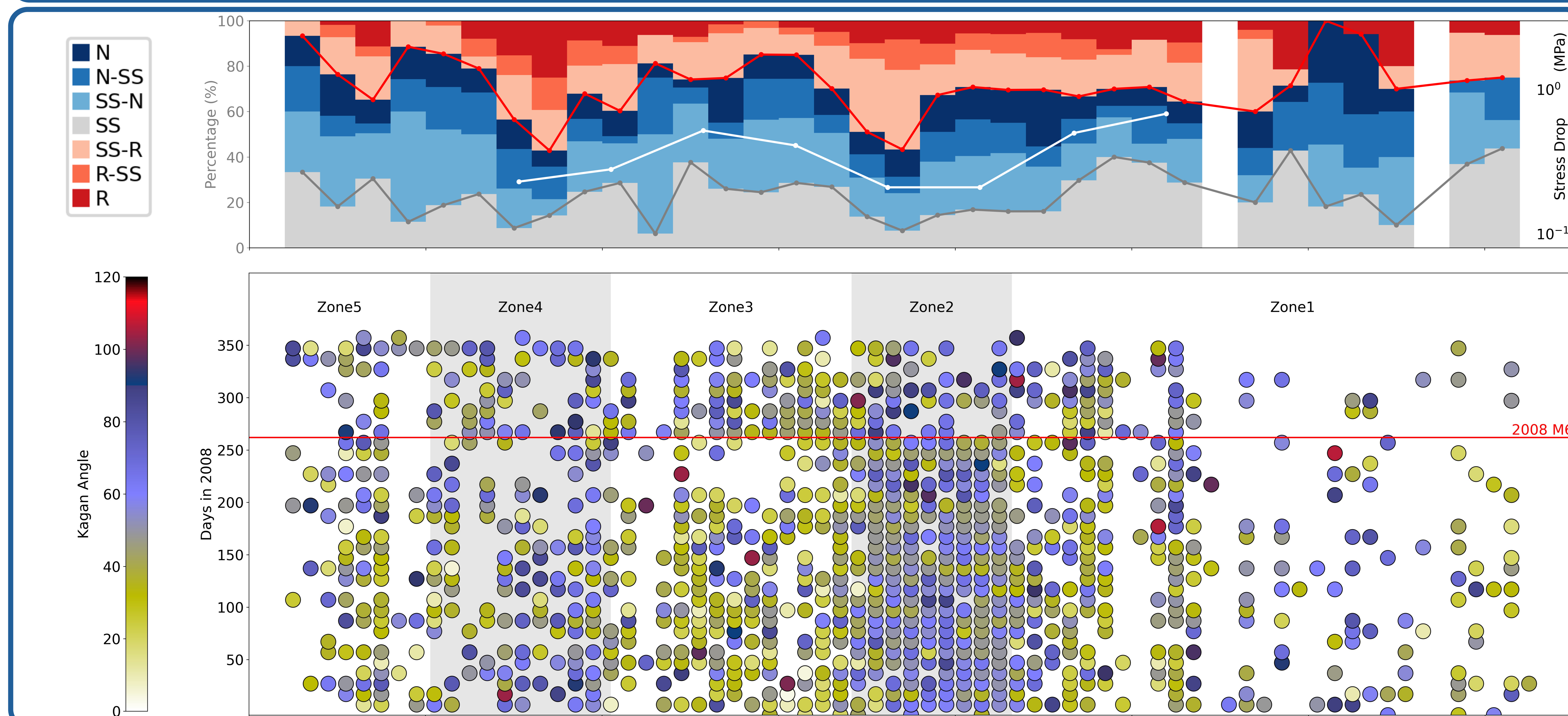
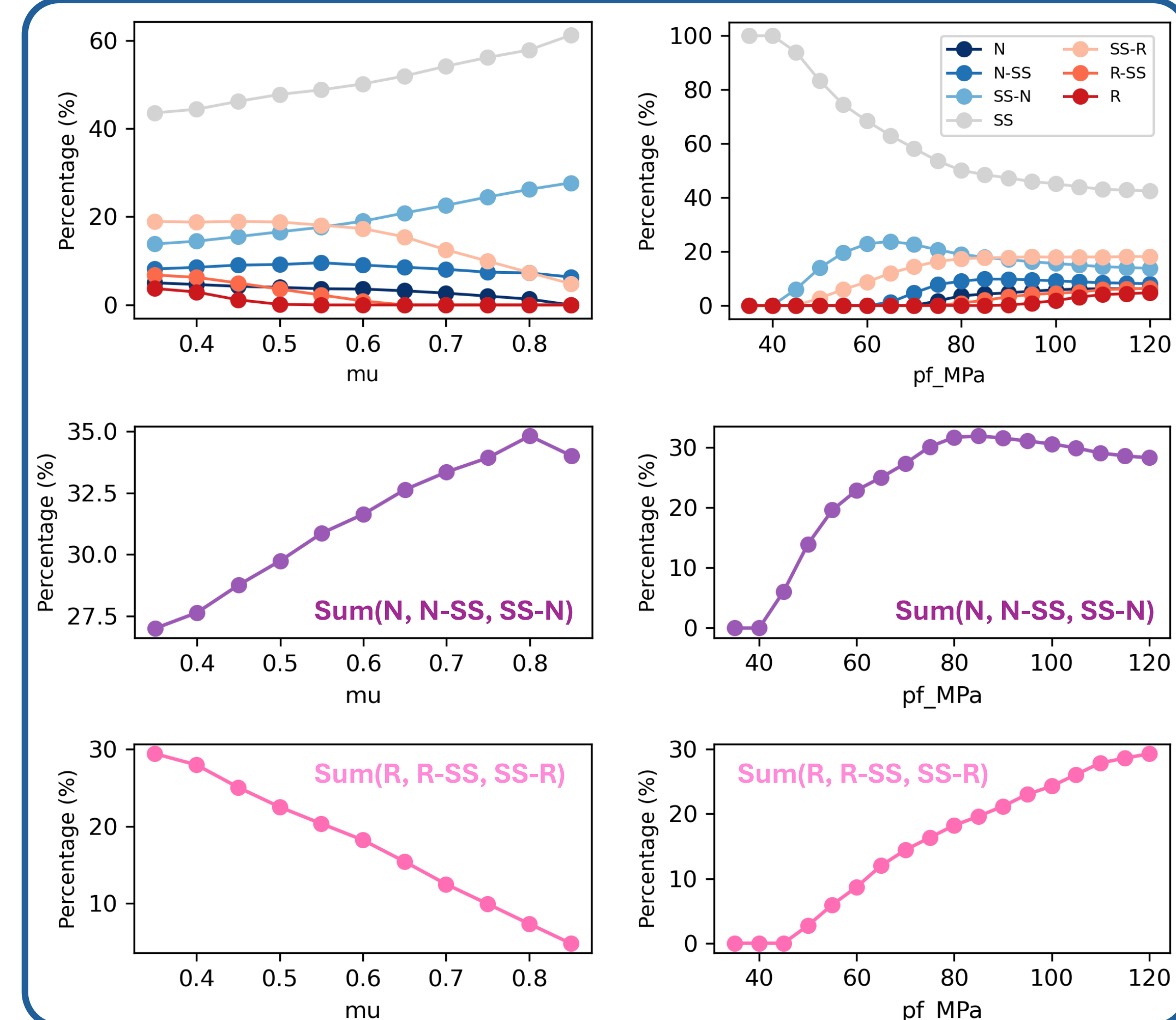


Abstract

Oceanic transform faults (OTFs) exhibit concurrent slip behaviors, combining creep with characteristic earthquakes restricted to localized patches. At the Gofar transform fault on the East Pacific Rise, magnitude (M) 6 earthquakes are bounded by creeping segments that act as persistent rupture barriers. However, physical controls of this segmentation remain unclear. Here, we analyze one year (2008) of ocean bottom seismometer data and develop a focal mechanism catalog of 3,122 earthquakes on the westernmost Gofar transform fault to investigate faulting style and stress regimes. Pure strike-slip earthquakes comprise only 20.5% of events; most are oblique, reverse, or normal earthquakes. These non-strike-slip earthquakes are broadly distributed, and their occurrence correlates with seismicity-inferred fault segmentation. Reverse and oblique-reverse events cluster within the long-term creeping barriers. Using Coulomb failure modeling, we interpret this pattern as evidence of elevated pore-fluid pressure and mechanical weakness within the rupture barriers. The 2008 M6 mainshock increased the focal mechanism diversity across the fault, indicating widespread secondary-structure activation. Our findings suggest that local mechanical properties govern slip mode and segmentation at Gofar, and likely other oceanic transform faults. Moreover, the prevalence of extension and compression reveals that these systems may behave as non-conservative plate boundaries within the oceanic crust.



Coulomb failure modeling



From spatial distribution of focal mechanisms

- Strike slip (SS), normal (N) and reverse (R) events are prevalent along the fault.
- Focal mechanisms suggest a uniformly distributed stress orientation along the fault.
- P-axes of R events closely align with the inverted σ_1 direction; T-axes of N events generally match the observed σ_3 direction with a $\sim 15^\circ$ deviation.
- Secondary structures are observed, such as the one shown with normal faulting events.
- Mainshock rupture zone has mechanisms more similar to the mainshock (smaller Kagan angle); rupture barrier zones have dissimilar mechanisms (larger Kagan angle).
- Percentage of SS events is high in rupture zones and low in barrier zones.
- Percentage of R, R-SS and SS-R events is high in barrier zones.
- Coulomb failure modeling indicates high R, R-SS and SS-R percentage and low SS percentage are related to low friction coefficient and high pore fluid pressure.
- Barrier zones have distinct subzones, with short 2–3 km patches having the highest pore fluid pressure, preventing the main rupture propagation.

From temporal distribution of focal mechanisms

- Focal mechanisms are less similar to mainshock after the mainshock in all zones.
- Inter-event Kagan angle increases after the mainshock in all zones, meaning focal mechanisms become more diverse.
- The increased diversity could be due to stress perturbations from the mainshock and/or a fault strength reduction caused by the mainshock.

Discussion

- Maximum principal stress at Gofar is $\sim 45^\circ$ from strike, differ from that of the San Andreas fault ($\sim 80^\circ$), indicating Gofar is generally stronger than San Andreas fault.
- Barrier zones are mechanically weak segments, creeping and bounding rupture zones, mirroring continental strike slip faults, such as San Andreas fault.
- Both extension and compression occur at seismogenic depths throughout the transform fault zone, with a prevalence of oblique normal events, implying that the system is not perfectly conservative.

References

- Tan et al. Variations in Mechanical Properties Control Segmentation of Oceanic Transform Faults. Under review.
- Gong & Fan (2022). Seismicity, Fault Architecture, and Slip Mode of the Westernmost Gofar Transform Fault. *JGR*.
- Kagan (2007). Simplified algorithms for calculating double-couple rotation. *GJI*.
- Álvarez Gómez (2019). FMC—Earthquake focal mechanisms data management, cluster and classification. *SoftwareX*.

Acknowledgements

- This work was funded by:
- NSERC postdoctoral fellowships 587558-2024
- NSF OCE-2527242
- SCEC 25260

